Acclimate—a model for economic damage propagation. Part 1: basic formulation of damage transfer within a global supply network and damage conserving dynamics

Robert Bierkandt · Leonie Wenz · Sven Norman Willner · Anders Levermann

Abstract Climate extremes are expected to become more frequent and intense under future warming. In a globalized economy, outages of productive capital and infrastructure have the potential to spread around the world. In order to address those repercussions in the framework of a risk analysis or a resilience strategy, a disaster's indirect consequences on the economic supply network need to be understood. We developed a numerical model to simulate these indirect effects along global supply chains for time scales of days to months. This article is the first in a series of four, which describes the damage-propagation model. In this first paper, we describe the pure damage propagation within the network and focus on the fundamental propagation of supply failure between production sites including their input and output storages and transport-related time delay. Idealized examples are presented to illustrate the dynamic damage propagation. Further articles will extend the dynamics to include demand changes due to the perturbation in the supply, the possibility to extend production to compensate for production failure, price responses and adaptive changes in the economic supply network. The underlying global supply network is based on data from multi-regional input–output tables. Transportation times are derived from geographic distances. In the initial model version presented here, indirect production losses are caused by cascading effects. They are propagated within the network without significant reduction in loss (damage conservation). They can thus be observed within the different storages or they "leak out" of the system through reduced consumption of the final consumer. As an example, we investigate the cascading behavior of losses for the machinery sector in Japan.

Keywords Climate change · Disaster risk · Extreme events · Economic networks · Damage propagations · Supply chain disruption

1 Introduction

Under future warming, extreme weather events, such as heat waves, droughts, mid-latitude storms, tropical cyclones, floods, and even extreme cold spells, are likely to intensify and become more frequent (IPCC 2013; Rahmstorf and Coumou 2011; SREX & IPCC). In a globalized world, where industries are linked in a complex and complicated way, extreme weather events might cause not only damages on regional productive capital and infrastructure, but also losses elsewhere along the supply chain (Levermann 2014). Besides the future evolution of extreme events, effective disaster risk management and resilience strategies (Linkov et al. 2005; Bridges et al. 2013; Linkov et al. 2014) depend on a robust understanding of indirect disaster consequences on the global economy.

R. Bierkandt · L. Wenz · S. N. Willner · A. Levermann
Potsdam Institute for Climate Impact Research (PIK),
Telegraphenberg A 31, 14473 Potsdam, Germany

R. Bierkandt · L. Wenz · S. N. Willner · A. Levermann
Institute of Physics, Potsdam University, Telegraphenberg A 31,
14473 Potsdam, Germany

L. Wenz
Mercator Research Institute on Global Commons and Climate
Change (MCC), Berlin, Germany

A. Levermann (✉)
Potsdam Institute for Climate Impact Research (PIK),
P.O. Box 601203, 14412 Potsdam, Germany
e-mail: anders.levermann@pik-potsdam.de

The severity of future climatic impacts on our society depends on the emission of carbon into the atmosphere (Levermann et al. 2011; World Bank 2012; IPCC 2014), which is represented by four representative concentration pathways (RCP) (Moss et al. 2010). Within the large variety of possible future impacts, those caused by climatic extremes are the most difficult to capture by scientific analysis due to their insufficient statistics, complex physical mechanisms (IPCC 2012, 2013), and societal responses (Hsiang et al. 2013; Helbing 2013; Brzoska and Scheffran 2013; Hsiang and Burke 2014). An important estimate of expected impacts of extreme weather events on various sectors in the EU was investigated within the PESETA II project (Ciscar Martinez et al. 2014). The damage related to tropical cyclones was estimated for the USA (Emanuel 2011; Zhai and Jiang 2014) and globally (Mendelsohn et al. 2012; Strazzo et al. 2013).

There is a wide range of research, which focuses on estimating direct losses caused by disaster (Auffhammer et al. 2006; Bouwer and Crompton 2007; Greenberg and Lahr 2007; Okuyama 2008; Hallegatte 2012) and some studies that also account for secondary effects of production losses (Okuyama 2008; Hallegatte 2008). An input–output framework was used to derive indirect losses after disasters, such as floods, tsunamis, or bombing in (Haddad and Okuyama 2012; Haddad and Teixeira 2013; Kajitani and Tatano 2014). Different initial strategies of including disaster-specific features in macroeconomic models, such as input–output models or computable general equilibrium models, are described by Okuyama and Santos (2014), and a review of the inclusion of climatic damages into integrated assessment models was provided by Lenton and Ciscar (2013). Indirect losses induced by the hurricane Katrina on a regional scale were estimated in an input–output framework including damage transfer dynamics as well as considering backward damage due to demand reduction as well as forward damage along supply disruptions (Hallegatte 2008). The ability of the economy to recover from those external exposed production outages was introduced as resilience strategies (Rose 2004).

This article proposes a dynamic damage-propagation model (denoted Acclimate hereafter) to assess the indirect effects of disasters on a global scale. Our approach distinguishes between (1) externally imposed direct losses, i.e., production losses due to damage of productive capital in the disaster area and (2) indirect losses, i.e., the reduction of production, caused by input losses. In contrast to (Hallegatte 2008), whose model is regionally confined, our approach considers the global supply network as a whole.

We present a series of four articles describing this damage-propagation model. This first one intends to investigate the basic response behavior in form of damage propagation after an external perturbation and its dynamical consequences. Like in Hallegatte's study (2008), an external perturbation reduces the production, assuming productive capital losses as a consequence of a disaster. Without external perturbation, production and consumption stay in the initial basic state, where we assumed the absence of seasonal fluctuations. We investigate the forward damage propagation along the supply chains on a time scale of days to month. In this model setup, it turns out that indirect production losses caused by cascading effects are either conserved in storages, propagated along the supply chain, or leak out of the system as consumption losses. In a physical analogy, there is no "diffusion" in the system and the damage is conserved. This kind of "damage diffusion" is introduced in the second article (Wenz et al. 2014b) in the form of production extension, which allows to produce more if the demand is increased. To this end, a demand dynamics is also included, which allows for an additional source of damage when demand is reduced due to reduced production in the wake of a disruption. This represents backward propagation of demand loss that turns into reduced production.

In this first version of the model, we assume that on short time scale (days to month), the response behavior can be approximated as availability limited, i.e., production sites respond to supply shocks, not to price shocks. In this version of the model, adjustment of prices for goods and services is not taken into account as response to a perturbation. This is clearly not the case in reality and will be exchanged by a price dynamics in the third article within the series.

At the core of the damage-propagation model, Acclimate, stand the decisions of economic agents on the rate of production, its distribution and consumption. In order to explicitly account for the effect of unanticipated perturbation, the model is not optimizing globally, but each agent optimizes its production locally. There are two types of economic agents: (1) production sites, representing industries in administrative regions and (2) consumption sites, representing the final demand of administrative regions. In this version of the model (excluding price dynamics), production sites (consumption sites) intend to sustain their initial production (consumption), which is considered to be optimal. The optimal value for the production and consumption is derived from data that are used to determine an initial basic state. Economic agents are assumed to have no foresight, meaning that they are not able to anticipate disasters and their consequences. Interactions between economic agents are described by the interplay of several nonlinear functions.

At the current level, production sites represent whole industries of an administrative region, which will be refined in later stages (Wenz et al. 2014a, b). Each administrative region is treated as a consumption site. Here the

consumption sites are the final consumers, i.e., household consumption, government spending, and investment.

We use data from multi-regional input–output tables (MRIOTs) to initialize a network of economic agents in Acclimate. We assume these data to represent a basic state of the global economy, representative of a specific year. The economic flows and production from the MRIOT are assumed to be the optimal state of the economic system, which is perturbed by external disruption and the consecutive damage propagation. In the presented version of the model, agents intend to return to this initial state as soon as the dynamics allows. For illustrative purposes and computation efficiency, administrative areas are considered only at a national level in this first approach. But we intend to refine those data to match the size of administrative regions with the size of disaster areas (Wenz et al. 2014a). The computation discussed in this article is based on MRIOTs provided by the EORA project that offers homogenized data tables for 26 commodity sectors in 186 countries from 1991 to 2011 (Lenzen et al. 2012).

One main assumption of this model (and its main nonlinearity) is that the production of a production site is limited by its inputs through the concept of perfect complementarity, i.e., production is limited by the strongest limitation of an input good or service that is necessary for the production. For example, if 10 % of one specific input is missing, then the production is reduced by 10 % unless another input is reduced by an even higher percentage (which would then determine the production reduction). To compensate for input failure, production sites can buffer a shortage by depleting the input storage of the respective good.

Here, we investigate the cascading effect of the forward propagation in the supply network, where the number of perturbed production sites increases with each affected site in a cascading way. The complimentary demand dynamics with backward propagation will be studied in the second article of this series Wenz et al. (2014b). A decision structure based on the price dynamics will be introduced in a third article and the network-adaptation dynamics in a fourth article.

This paper is structured as follows: In Sect. 2, we present the numerical damage-propagation model Acclimate. After having described how we initialize the basic state of the global supply network with data from multi-regional input–output tables, we introduce the dynamics of production, storage, and consumption. In Sect. 3, we assume that the Japanese manufacturing sector stops production for several days and investigate the response of the globally aggregated production level. We analyze the response as a function of the perturbation period, and we derive a critical perturbation length above the network experiences cascading production losses. We present our conclusions in Sect. 4.

## 2 Basic formulation of damage propagation within a global supply network

This section presents the numerical damage-propagation model, Acclimate, which can be used to simulate global dynamic repercussion in the aftermath of local production outages. Firstly, we present agents (production sites and consumption sites) as the constituents of the global supply network and discuss how we initialize those in the model with data from multi-regional input–output tables. Secondly, we present the agent's decision options and intentions on production, distribution, and consumption. Thirdly, we describe the evolution of production and storage under external perturbations.

2.1 Basic network: global supply flows from multi-regional input–output tables

First we need to initialize the global supply network with data. The global supply network represents the entirety of production and consumption sites and all links, i.e., commodity flows, between them. Commodities are marketable items to satisfy wants and needs and comprise goods and services. While production sites use distribute and produce commodities, consumption sites merely consume without further output. The economic quantities within the network will evolve in time around the initial network as perturbations are introduced. As detailed below, the dynamics as represented here will tend to restore the initial economic network.

Consider a production site denoted by the indices i and r, where i refers to the commodity, i.e., the good or service produced, and r denotes the region. This production site ir is connected to other production sites js via output flows $Z_{ir \to js}^{(t)}$ and input flows $Z_{js \to ir}^{(t)}$. Flows between production sites are intermediate flows that are used for further production. Time is represented by t and measured in units of days. A consumption site is attached to each of the regions, and we treat consumption sites as a sector j_f in region s. A flow $Z_{ir \to j_f s}^{(t)}$ indicates a final demand flow from a production site ir to consumption site $j_f s$. By definition, consumption sites have only ingoing flows and no outgoing flows. Flows are given in units of nominal US \$ per time and their definition follows Peters et al. (2011).

We use MRIOTs to initialize the commodity flows $Z_{ir \to js}^{(t=0)} = Z_{ir \to js}^*$, where the index j includes consumption sites j_f. MRIOTs comprise commodity flows per year for

Input-Output Tables

Global Supply Network
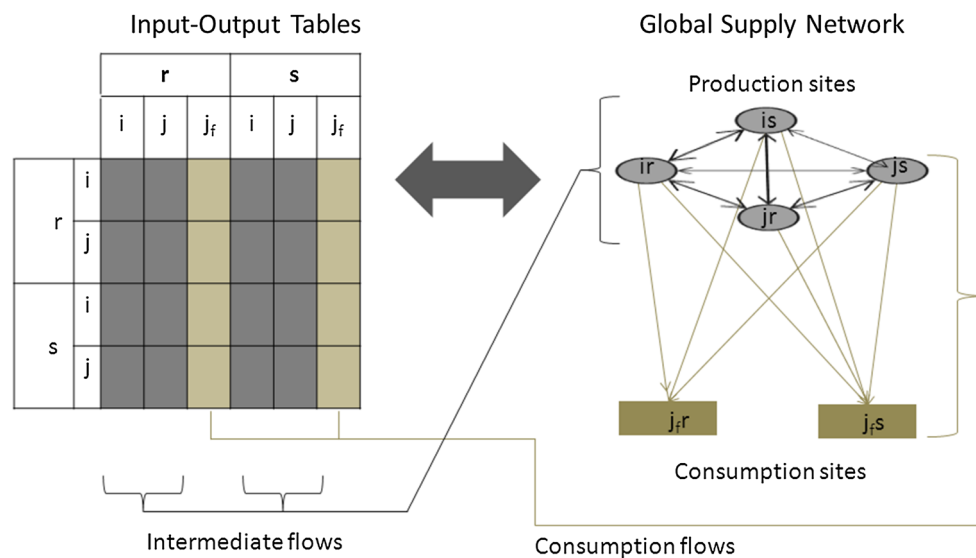
Fig. 1 Schematic illustration of a multi-regional input–output table (MRIOT) (*left*) that represents the global supply network (*right*). Both illustrations represent the same network of economic independencies and are exchangeable representations of the economic network. A MRIOT serves as a basis for the damage-propagation model Acclimate. Above a world with two regions r and s is considered. Each region has a consumption site j_f as well as production sites of two commodities, i.e., goods and services, i and j. If every field of the table is nonzero, then production sites in the supply network form a fully connected bidirectional sub-network. The consumption sites of the regions are coupled unidirectionally to all production sites, i.e., consumption sites have only ingoing flows. This scheme can easily be generalized to multiple regions and sectors. Generally, not all production sites are interconnected, i.e., the matrix is relatively sparse

various industries of administrative entities, which commonly represent countries or groups of countries. The construction of global MRIOTs was undertaken by projects like GTAP (Narayanan et al. 2012), WIOD (Dietzenbacher et al. 2013), and EORA (Lenzen et al. 2012). Multi-regional supply and use tables for the EU were created by EXIOPOL (Tukker et al. 2013). The construction of an MRIOT from GTAP data is described by Peters et al. (2011) and Andrew and Peters (2013).

MRIOTs provided by the EORA project offers homogenized data tables for 26 commodity sectors in 186 countries from 1991 to 2011 (Lenzen et al. 2012). We used the EORA data to construct a basic network at country level. Since disasters are regionally confined, we will eventually need a higher regional resolution than the national level to investigate climate change impacts. To this end, we apply the disaggregation method by Wenz et al. (2014a) on EORA-MRIOTs to down-scale the data to higher sectoral and regional detail in future studies. In order to be computationally efficient and illustrate the damage propagation, we stay on the national level for this study here.

In addition, the community project Zeean (www.zeean.net) was launched to collect data on global supply chains (Levermann 2014). As a community effort, Zeean aims to improve the representation of economic flows. Possible conflicts from different data inputs are resolved by open-source algorithms as described in (Wenz et al. 2014a, b).

Figure 1 illustrates the construction of a global supply network from an MRIOT for a fully connected world with only two regions and two sectors in each of those regions. The commodity indices i, j represent industrial sectors and r, s the corresponding administrative regions at country level. Each region represents a consumption site, $j_f r$ and $j_f s$, with ingoing flows only. Production sites ir, jr, is, and js are fully connected in this example. MRIOT and global supply network are equivalent representations and exchangeable. This approach can be easily generalized for more regions and sectors. In general, not all production sites will be interconnected.

We converted the data of the year 2011 from flows per year to flows per day and assumed that no seasonal fluctuations occur. This can be easily refined in future applications. The MRIOT defines our initial state that we assume to be the desired basic state of the global supply network.

It is important to note that we do not attempt to model the evolution of the global economic network but assume this to be represented by the MRIOT. The damage-propagation model, Acclimate, operates as an anomaly model around the desired state, which propagates damages within the economic model. That is to say, in the absence of perturbations, the global supply network sustains in the (basic) initial state.

During the harmonization of MRIOT, a number of smaller flows are introduced to balance the matrix. These
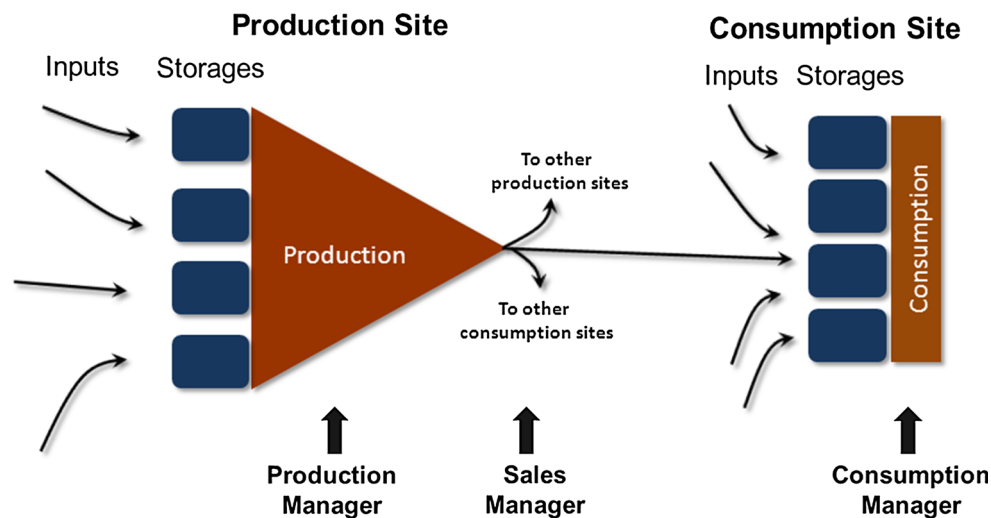
Fig. 2 Production sites and consumption sites constitute a global supply network and are the economic agents of our model, which aim toward their optimal production and consumption value as given by the MRIOT. All agents are equipped with storages to buffer supply failures. Agent's decisions on production, distribution and consumption are committed to production, sales, and consumption managers, respectively. Production and consumption managers take storages into account to aim toward their initial production and consumption values. External perturbation reduces production capacities of individual production sites in the network

flows are not necessarily realistic and in general lead to a fully occupied MRIOT. In our agent-based approach, these small but potentially unrealistic flows are relevant because they can spread damage in a potentially unrealistically diluted manner. At the same time, it reduces the computational performance of the model dramatically. We thus introduced a threshold flow of 10^6 US \$ and neglected all flows that are smaller, assuming that they might not be realistic. This threshold is set in an arbitrary way, and all results obtained with the model should be scrutinized with respect to variations of this threshold. The threshold will become less relevant with an improved database as envisaged by the Zeean project.

2.2 Agent's decisions on production, distribution, and consumption

The dynamics of the model is driven by decisions of economic agents on production and product distribution and consumption. The optimal value for production and consumption is derived from data that are used to determine the basic state. Economic agents are assumed to have no foresight, i.e., they are not able to anticipate disasters and their consequences. This assumption can be relaxed in future versions of the model but is used as a starting point to investigate responses of low-probability extreme events that are unanticipated. In principle, storage capacities in the model allow agents to be prepared for supply disruptions. However, since storage-holding is costly, just-in-time productions with minimized storage capacities are attractive in global production processes. The storage size is a

parameter of each agent and can thus be subject of future sensitivity studies.

Here we present the decision making for production and consumption sites. All economic agents, production sites as well consumption sites, are equipped with storages for input goods, which are used to buffer supply shortages. See Fig. 2 for an illustration. A list for all quantities and parameters is given in Table 1.

The production of a production site is its total output per time step at time t,

$$X_{ir}^{(t)} = p_{ir}^{(t)} X_{ir}^*, \quad (1)$$

and depends on the production ratio $p_{ir}^{(t)}$. The initial output of production site ir described by X_{ir}^* is set equal to the total sum of all outgoing flows, $X_{ir}^* = \sum_j \sum_s Z_{ir \to js}^*$, of the MRIOT.

The initial production ratio, $p_{ir}^{(t=0)} = p_{ir}^*$, is assumed to be optimal, and production sites intend to reach its initial production ratio at each time step. However, the production of ir may be reduced for two reasons: First, directly by an adverse event destroying parts of ir's productive capital or secondly, indirectly by supply shortages. In either case, production sites will apply the maximum production ratio possible. Thereby, the production ratio,

$$p_{ir}^{(t)} = \hat{p}_{ir}^{(t)}, \quad (2)$$

is determined by the possible production ratio $\hat{p}_{ir}^{(t)}$, which takes into account the available amount of inputs and storages at time t and reductions of production in the disaster aftermath.

Table 1 Overview of all quantities and parameters used in the model in order of appearance

Quantity/ parameter	Meaning	Unit
$Z_{ir \to js}^{(t)}$	Intersectoral flow	Quantity/ Time
$Z_{ir \to j_f s}^{(t)}$	Final demand flow	Quantity/ Time
$X_{js}^{(t)}$	Production	Quantity/ Time
$p_{js}^{(t)}$	Production ratio	Ratio
$\hat{p}_{js}^{(t)}$	Possible production ratio	Ratio
$C_{i \to j_f s}^{(t)}$	Consumption	Quantity/ Time
$c_{i \to j_f s}^{(t)}$	Consumption ratio	Ratio
$\hat{U}_{i \to js}^{(t)}$	Possible used flow	Quantity/ Time
$U_{i \to js}^{(t)}$	Used flow	Quantity/ Time
$\lambda_{js}^{(t)} \in [0,1]$	Forcing on production site	Ratio
$\hat{C}_{i \to j_f s}^{(t)}$	Possible consumption flow	Quantity/ Time
$\lambda_{i \to j_f s}^{(t)} \in [0,1]$	Forcing on production site	Ratio
$I_{i \to js}^{(t)}$	Input flow	Quantity/ Time
$S_{i \to js}^{(t)}$	Input storage	Quantity
Δt	Time step for numerical computation	Time
$\mu_{i \to js}^{(t)} \in [0,1]$	Forcing on storage	Ratio
$\omega_i \geq 1$	Upper storage limit	Ratio
ψ_j	Storage fill factor	Ratio
$T_{ir \to js}^{(t)}$	Transport stock	Quantity
$T_{ir_b \to js}^{(t)}$	Transport section stock	Quantity
$\tau_{ir \to js} \geq \Delta t$	Transit time	Time

Production sites do not only produce, they also decide on distribution of their output commodities. As a first very simple strategy, we assume that they distribute their share of output equally over time among all purchasers, i.e., the ratio

$$\frac{Z_{ir \to js}^{(t)}}{X_{ir}^{(t)}} = \frac{Z_{ir \to js}^{*}}{X_{ir}^{*}} = \text{const.} \rightarrow Z_{ir \to js}^{(t)} = \frac{Z_{ir \to js}^{*}}{X_{ir}^{*}} X_{ir}^{(t)}, \quad (3)$$

is kept constant to the initial value given by the basic state. Since any production loss is distributed equally among the buyers, we call this decision approach equal distribution. The role of this strategy and other possible strategies is discussed in the second article (Wenz et al. 2014a, b).

Final demand comprises all commodity flows that represent household consumption, investment, and government spending, but excludes use for further production. Agents who capture those flows are defined as consumption sites. Since those consumption sites merely consume commodities without further output, they are connected to production sites via input flows only as illustrated in Fig. 2. Like production sites, consumptions site are equipped with storages, and in the following, we will treat consumption sites as a sector i_f in region r. Analogously to production sites, consumption site i_f in region r intends to keep or reach its initial consumption $C_{j \to i_f r}^{*}$ of commodity j to the amount that is possible,

$$C_{j \to i_f r}^{(t)} = c_{j \to i_f r}^{(t)} C_{j \to i_f r}^{*}. \quad (4)$$

The consumption ratio $c_{j \to i_f r}^{(t)}$ takes into account the available amount of inputs and storages of commodity j at time t.

2.3 Time evolution of production and storage

In this subsection, we describe the time evolution of the production flow and storage content, and we introduce external perturbations on production and storage capacities.

The evolution of the production $X_{ir}^{(t)}$ of production site ir in the network is determined by the production ratio $p_{ir}^{(t)}$ in Eq. (1). From Eq. (2), it follows that agents intend to keep the production ratio at the initial value or the maximum value that is possible, i.e., $\hat{p}_{ir}^{(t)}$. An external perturbation ratio, $0 \leq \lambda_{ir}^{(t)} \leq 1$, can be imposed on the possible production ratio $\hat{p}_{ir}^{(t)}$. This forcing describes a perturbation of the initial basic state. In absence of any perturbation, this ratio is unity and describes, in the case of sufficient supply, an upper limit of the production ratio.

We start from Eq. (2) and specify all quantities necessary for the computation of the production ratio that is possible, i.e., $\hat{p}_{ir}^{(t)}$. The latter depends on inputs and storage contents of commodities at time t that are available for production and is given by

$$\hat{p}_{ir}^{(t)} = \min \left(\min_j \left(\frac{\hat{U}_{j \to ir}^{(t)}}{U_{j \to ir}^{*}} \right), \lambda_{ir}^{(t)} \right). \quad (5)$$

Here, $U_{j \to ir}^{*}$ describes the initial used flow, i.e., the amount of a commodity j used per time step for production of commodity i by production site ir in the basic state. The maximum used flow that can, under current input flows and available storage content, be used for production is denoted as the possible used flow $\hat{U}_{j \to ir}^{(t)}$.

In Eq. (5), the minimum condition with respect to the different commodities j reflects the assumption of perfect complementarity. This is a key assumption in our model and states that the production of output commodity i

requires the availability of all necessary input commodities j in specific quantities. If one input commodity is not available for production, the entire production has to be interrupted. Therefore, the possible output is constraint by the minimum of ratio $\hat{U}_{j \to ir}^{(t)}/U_{j \to ir}^*$ among all required input commodities j. The assumption of perfect complementarity represents the strongest nonlinearity in the model.

The consumption site's consumption ratio for commodity j,

$$c_{j \to i_f r}^{(t)} = \min \left(\frac{\hat{C}_{j \to i_f r}^{(t)}}{C_{j \to i_f r}^*}, \lambda_{j \to i_f r}^{(t)} \right), \tag{6}$$

is determined by the possible consumption $\hat{C}_{i \to i_f r}^{(t)}$ of commodity i by consumption site $i_f r$. An external perturbation on the consumption can be imposed by the parameter $0 \leq \lambda_{j \to i_f r}^{(t)} \leq 1$.

The maximum flow of commodity j that can be used for production, i.e., the possible used flow in Eq. (5), or consumption, i.e., the possible consumption flow in Eq. (6), at time step t are given by

$$\hat{U}_{j \to ir}^{(t)} = I_{j \to ir}^{(t)} + \frac{S_{j \to ir}^{(t)}}{\Delta t} \text{ and } \hat{C}_{j \to i_f r}^{(t)} = I_{j \to i_f r}^{(t)} + \frac{S_{j \to i_f r}^{(t)}}{\Delta t}, \tag{7}$$

respectively.

The possible used flow and possible consumption flow depend on how much j is stored, i.e., the storage content for $S_{j \to ir}^{(t)}$ and the input flow of j, i.e., $I_{j \to ir}^{(t)}$, at time t. Consumption sites $i_f r$ are incorporated by index i in all quantities from now on. Dividing the storage content by the time step Δt yields a flow, i.e., $[S/\Delta t]$ = quantity/time.

The available storage content $S_{j \to ir}^{(t)}$ at time t in Eq. (7) is derived from the previous input flow $I_{j \to ir}^{(t-1)}$ and used flow $U_{j \to ir}^{(t-1)}$ and is therefore given by

$$S_{j \to ir}^{(t)} = \max \left(\min \left(\mu_{i \to js}^{(t)} \omega_i S_{j \to ir}^*, S_{j \to ir}^{(t-1)} + \Delta t \left(I_{j \to ir}^{(t-1)} - U_{j \to ir}^{(t-1)} \right) \right), 0 \right). \tag{8}$$

The storage content is always positive, and an external perturbation of the storage content can be imposed by the forcing parameter $0 \leq \mu_{i \to js}^{(t)} \leq 1$. An upper storage limit is given by the ratio $\omega_j \geq 1$. The storage content of the basic state $S_{j \to ir}^* = \psi_j \cdot I_{j \to ir}^*$ is derived from the basic-state input flow $I_{j \to ir}^*$ and the storage fill factor ψ_j and defines the initial storage content $S_{j \to ir}^{(t=0)} = S_{j \to ir}^*$. A storage fill factor of $\psi_j = 3$ for all input commodities j ensures that production sites can overcome supply failures that last not more than 3 days. In an undisturbed system, input flows $I_{j \to ir}^{(t)}$ and used flows $U_{j \to ir}^{(t)}$ are equal, and the storage content $S_{j \to ir}^{(t)}$ remains constant.

After having determined the storage content in Eq. (7), we need to compute the input flow $I_{j \to ir}^{(t)}$ in Eq. (7). Input flow $I_{j \to ir}^{(t)}$ is the amount of commodity j reaching ir at time t. We further introduce a transport-induced time delay $\tau_{js \to ir}$ that accounts for the transit time, required for good j to be transported from region s to production site ir. In general, transit times $\tau_{ir \to js}$ are sector specific and depend on interregional distances. Here we neglect the sector dependence. Transit times are given in multiples of days and depend only on the regions.

To estimate those region-to-region transportation times, we used geographic distances between the capitals of the countries and average velocities of transport mediums. Average vessel and truck speed are given by 26 km/h (14 knots) and 45 km/h (SEARATES LP SEARATES 2014). For distances below 3,000 km, we considered average speed of trucks and above 3,000 km average vessel speed. We need to consider that real trajectories using roads and waterways are always larger than geographic distances. In addition, even if 45 km/h is given as default value at sea-rates.com for truck speed, there might be regulation issues to breaks and sleeping times of truck drivers that lowers the average speed. Therefore, we reduce the average vessel speed to 20 km/h and the average truck speed to 35 km/h. While we focus here primarily on the mechanism of damage-propagation, transportation times might need further attention for future applications of the model.

During simulations with Acclimate, there will be a certain amount of goods in transportation. These stocks of goods are located between two interconnected production or consumption sites. In our model, this transport stock, i.e., the total amount of goods located between production site js and ir (or consumption site $i_f r$) at time t, is represented by a vector $T_{js \to ir}^{(t)}$. This connection is only defined by source, target, and transit time. Using this information, we split the total transport stock $T_{js \to ir}^{(t)}$ into $\tau_{ir \to js}$ discrete transport sections, and the content of each transport section moves forward the supply chain by one section per time step until it reaches the purchaser. This concept enables us to implement a destruction of infrastructure and goods during transportation as external perturbation at a later stage of model development. Hence, the transport stock is the sum of all transport stock sections between js and ir

$$T_{js \to ir}^{(t)} = \sum_{b=0}^{\tau_{js \to ir}-1} T_{ir \underset{b}{\to} js}^{(t)}, \tag{9}$$

where b denotes the individual transport section.

The amount of goods in an arbitrary transport section b depends on the output flow sent from the producer at time $t - b$,

$$T_{\substack{js \to ir \\ b}}^{(t)} = Z_{js \to ir}^{(t-b)} \Delta t, \quad \forall b \in \left[0, \tau_{js \to ir} - 1\right]. \tag{10}$$

The flow in Eq. (10) between js and ir at time $t - b$,

$$Z_{js \to ir}^{(t-b)} = \frac{Z_{ir \to js}^*}{X_{ir}^*} X_{js}^{(t-b)}, \quad \forall b \in \left[0, \tau_{js \to ir} - 1\right], \tag{11}$$

is computed with the production $X_{js}^{(t-b)}$ at time $t - b$ and the constant distribution ratio $\frac{Z_{ir \to js}^*}{X_{ir}^*}$ from Eq. (3).

The input flow $I_{j \to ir}^{(t)}$ of Eq. (7) is then obtained by summing the contents of the last transport sections over all ingoing transport connections,

$$I_{j \to ir}^{(t)} = \frac{1}{\Delta t} \sum_{s'} T_{\substack{js' \to ir \\ b(s)}}^{(t)}; \quad b(s) = \tau_{js \to ir} - 1, \tag{12}$$

where we used all the final transport sections of all ingoing transportation connections. In other words, the flow out of the last transport section becomes the input flow of the receiving agent. With Eqs. (8) and (12), we are now ready to compute the possible used flow $\hat{U}_{j \to ir}^{(t)}$ for the production from Eq. (7) and eventually the possible production ratio $\hat{p}_{ir}^{(t)}$, which equals, according to Eq. (2), the actual production rate $p_{ir}^{(t)}$.

The used flow for production sites is computed according to

$$U_{j \to ir}^{(t)} = p_{ir}^{(t)} U_{j \to ir}^*. \tag{13}$$

The consumption flow of consumption site $i_f r$ at time t equals its used flow

$$C_{j \to i_f r}^{(t)} = U_{j \to i_f r}^{(t)} = c_{j \to i_f r}^{(t)} U_{j \to i_f r}^*. \tag{14}$$

The computation of the time step t is completed and can be done for the next time step, i.e., $t = t + \Delta t$.

The model is implemented in C++.[1] The following simulations are based on a representation of the global supply network derived from multi-regional input–output data for the year 2011. The data are provided by EORA (Lenzen et al. 2012) and describe annual economic flows in US $ between 27 sectors in 186 regions. Consequently, the network consists of 5,022 nodes, where 4,836 nodes can be interpreted as production sites and 186 as consumption sites. The network consists of 500×10^3 links that represent annual commodity flows above 1 million US $. As mentioned above, we neglected all smaller flows in the data, assuming that flows below this magnitude are negligible. For the standard output setting, it takes on average 1 min on a 1.8 GHz kernel computer to compute 1 year if the duration of each time step equals 1 day.

---

[1] Code is available upon request.

3 Examples of damage and loss propagation in response to local production failure

In this section, we apply the model Acclimate to a specific idealized production outage scenario and investigate the global damage propagation. First, we investigate direct and indirect losses after the disruption of the Japanese "machinery" sector, then we define aggregated flow and stock quantities that are useful in understanding damage propagation within Acclimate and investigate the temporal evolution of those global quantities, and thirdly, we follow specific supply chains. In these steps, we make special use of the lack of damage diffusion. Finally, we examine cascading behavior of production losses and investigate conditions under which a cascade propagates. We distinguish between damages and losses. Damages apply to stock quantities, i.e., stored and transported commodities as well as productive capital like factories, while losses apply to flow quantities, i.e., productive flows, input flows, used flows, and consumption flows. Cascading behavior occurs if production losses of one production site cause other production sites to stop or reduce their production. Cascading production losses are always indirect losses. A cascade of first order is caused by direct production loss of a perturbed production site.

3.1 Direct and indirect damages and losses after the disruption of the Japanese "machinery" sector

We perturb the global supply network by setting the production ratio of one production site to zero. We choose Japan's "machinery" sector, since it is well connected within the global supply network and very exposed to natural hazards. As a sample perturbation, we choose a complete shutdown for periods between 1 and 30 days. Storages size and external perturbation parameters are given in Table 2. We neglected all self-loops, i.e., supply for a production site that is also its output, to focus only on the interactions between production sites.

For the simulation, we assume that all commodities are storable goods, i.e., we do not distinguish between goods and services. For all storages of production and consumption sites, we select a fill factor of $\psi_j = 3$, i.e., each economic agent has enough goods stored to continue the production even if no supply is obtained for 3 days. The underlying basic global supply network is based on input and output data for 2011 (Lenzen et al. 2012). The perturbation parameter on the production ratio, $\lambda_{ir}^{(t)}$, for the machinery sector in Japan is set to zero for different outage times. This corresponds to a direct global production reduction of 0.8 %. While the externally imposed

Table 2 Storages size and perturbation parameters for the example of a disruption of the Japanese "machinery" sector

Parameters for storage and perturbation	
$\psi_j = 3$	Storage fill factor
$\omega_i = 1$	Upper storage limit
$\lambda_{js}^{(t)} = 0, \quad j = \text{MACH}, \quad s = \text{JPN}, \quad t_i \le t \le t_i + t_{\text{pert}}$	Perturbation on the production ratio of the Japanese machinery sector for perturbation period t_{pert}
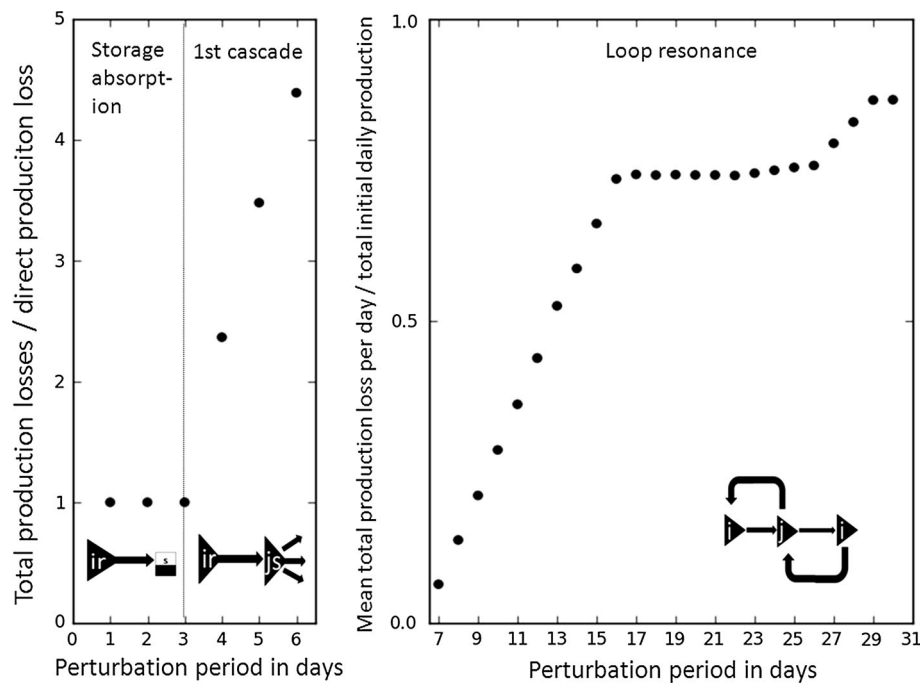
Fig. 3 The globally aggregated total production loss over the induced direct loss for different lengths of perturbation periods for a complete shutdown of the Machinery sector in Japan. Up to a perturbation period of 3 days, no indirect losses occur due to the chosen storage size. If an external perturbation is imposed for more than 3 days, a production loss cascade is triggered, and if the outage lasts more than 6 days, the global aggregated production level does not return to the initial value but oscillates due to resonance loops and the absence of diffusion. Up to 6 days of perturbation, a recovery of the total production level to the initial value occurs after the perturbation is ceased. The *left panel*, the total production loss, i.e., direct and indirect loss, in units of direct production loss due to a perturbation. The *right panel*, the mean total production per day in units of the initial total production

production loss (here the outage of the Japanese "machinery" sector) is denoted as direct loss, the production loss that occurs in consequence of supply disruptions is referred to as indirect loss.

Figure 3 presents the total production loss, i.e., the sum of direct and indirect production loss, in units of direct production loss. We observe three different regimes of the response: (1) no indirect loss, i.e., total loss equals direct loss (1–3 days of production outage), (2) the ratio of total production loss to direct loss increases with the direct loss (4–6 days of production outage), (3) an oscillating production loss where a recovery of the initial production level is not possible (7–30 days of forced production outage). In the oscillatory regime, the production does not return to its initial state even after the perturbation has ceased. That is why, the ratio between

the mean total production loss per day and the initial global production is plotted as a function of the length of perturbation period. This oscillatory behavior depends on a number of parameters and will be discussed in the next sections.

3.2 Tracking damages and losses along the global supply network: an aggregated perspective

To explain the three different kind of response behavior observed in Fig. 3, we investigate and discuss the damage and loss transfer between globally aggregated flow and stock quantities. Taking this macroscopic perspective, we are, for the moment, only interested in global quantities and do not regard propagation dynamics between individual production and consumption sites.
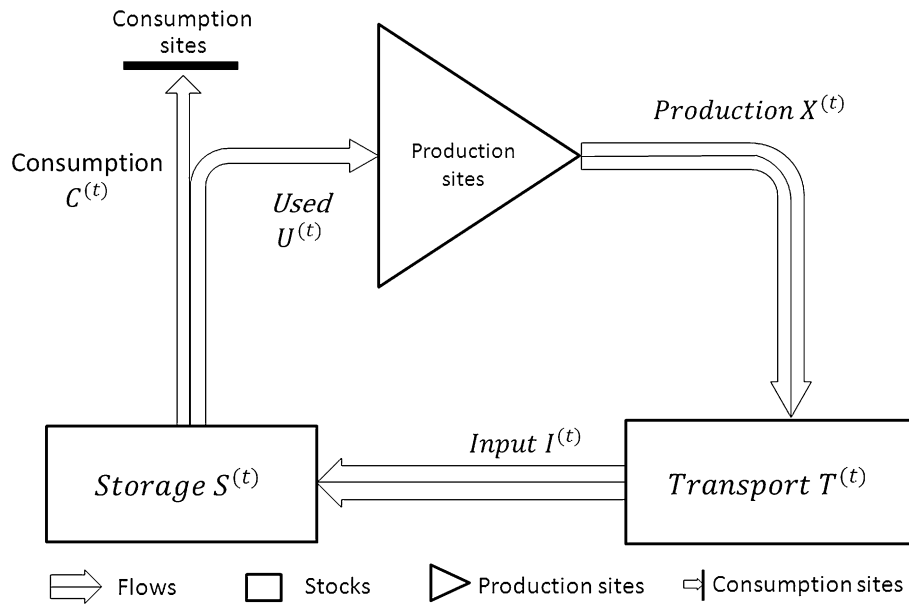
Fig. 4 A stock and flow model for the global aggregated supply network. *Arrows* and *boxes,* globally aggregated flows and stocks of commodity values, respectively. Production sites amplify the value of global used flow $U^{(t)}$, and consumption sites represent a sink for the global consumption flow $C^{(t)}$. The Global output of production sites, i.e., global production $X^{(t)}$, enters the global transport stock $T^{(t)}$, where it stays for site specific transportation times and flows as global input flow $I^{(t)}$ into the storage stock of production and consumption sites. Globally aggregated storage contents are denoted as $S^{(t)}$. The center line in $X^{(tt)}$ and $I^{(t)}$ separates intermediate flows, which form a cycle together with $U^{(t)}$, and final flows, which leave the cycle toward

consumption sites, which serve as a sink of the flow. In the (initial) basic state, global production flow, global input flow, and the sum of global consumption and global used flow are of the same size. A perturbation of the production of one or more production sites leads to direct production loss and causes indirect loss, if the direct loss reaches other production sites. The transport stock acts as loss delayer with corresponding transportation times. Storage stocks serve as buffer and can absorb input loss if sufficient storage content is available. In other words, available storage contents prevent indirect losses to propagate to production sites or to consumption sites

Figure 4 illustrates the globally aggregated flows and stocks in the network. The global production flow $X^{(t)}$, the global input flow $I^{(t)}$, the global used flow $U^{(t)}$, and the global consumption flow $C^{(t)}$ are obtained by summation over all sectors and regions,

$$X^{(t)} = \sum_i \sum_r X_{ir}^{(t)}, \quad I^{(t)} = \sum_j \sum_i \sum_r I_{j \to ir}^{(t)},$$
$$U^{(t)} = \sum_j \sum_i \sum_r U_{j \to ir}^{(t)}, \quad C^{(t)} = \sum_j \sum_r C_{j \to i_f r}^{(t)}. \quad (15)$$

In the basic state, i.e., in the absence of direct and indirect production losses, the following equality holds:

$$X^{(t)} = I^{(t)} = U^{(t)} + C^{(t)}. \quad (16)$$

Transport sections and storage contents are aggregated stocks of goods,

$$T^{(t)} = \sum_i \sum_r \sum_j \sum_s T_{ir \to js}^{(t)}, \quad S^{(t)} = \sum_i \sum_j \sum_s S_{i \to js}^{(t)}, \quad (17)$$

where the summation over sectors j includes the final demand and thus transport stocks and storages of the consumption sites.

The global supply network can be characterized by the set of flow and stock quantities illustrated in Fig. 4. Furthermore, Fig. 4 illustrates the propagation cycle of commodities in the global supply network. We can interpret the arrows as flows and the squares as stocks. Commodity flows feed commodity stocks and vice versa. Commodities, in units of US \$, move along the arrows of Fig. 4 until they are consumed by consumption sites or transformed by production sites to new commodities. A perturbation of production $X^{(t)}$ causes direct production losses. We expect this loss to propagate along the arrows of Fig. 4 in a similar fashion. The transport stock $T^{(t)}$ delays the arrival of the loss because of transit times. Storages $S^{(t)}$ serve as buffer by absorbing supply failures, which reach the storages as input losses. If storage contents are not sufficient, losses arrive at consumption sites or yield a production loss at another production site. Whether such an amplification of losses occurs depends on the size of storage contents, the imposed perturbation strength, and its length.

The dynamic evolution of all global flows and stocks for a set of perturbation periods from Fig. 3 is illustrated in Fig. 5. The left column, Fig. 5a, shows the response of the
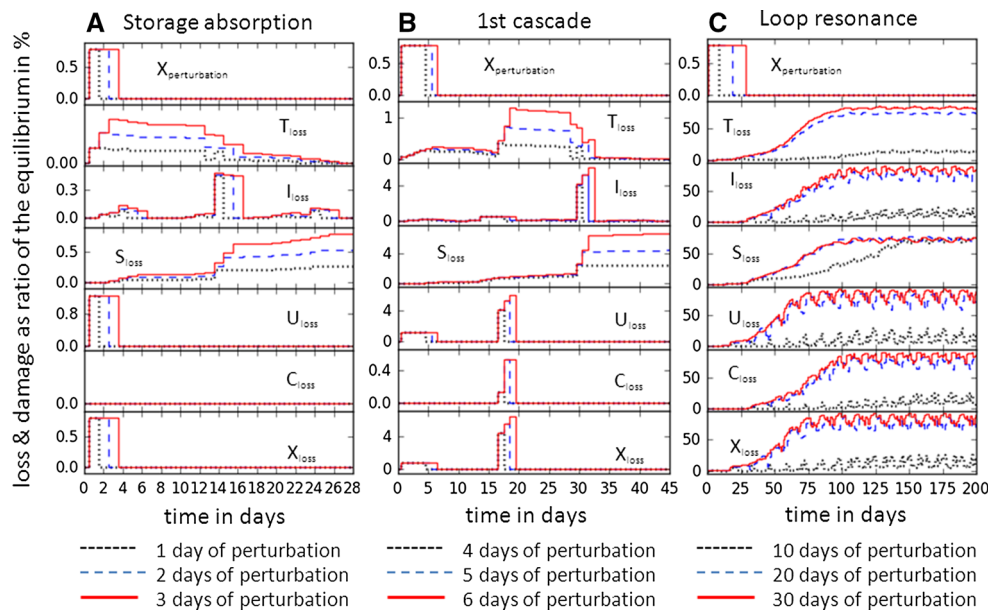
Fig. 5 Dynamic evolution of damages and losses as relative deviation from equilibrium for globally aggregated quantities in response to nine different perturbation lengths. Each *row* represents the deviation of one global flow or stock quantity. Quantities are ordered accordingly to the flow direction of Fig. 4 and start with the perturbed production loss $X_{perturbation}$ as deviation from the global production. The subsequent rows represent the deviation ratio of transport stock

T_{loss}, input flow I_{loss}, used flow U_{loss}, consumption flow C_{loss}, and production flow X_{loss}. Three regimes can be distinguished for the production flow X_{loss}, depending on the length of the imposed perturbation: **a** X_{loss} is equal to the perturbed production due to storage absorption of losses, **b** it exhibits cascading losses or **c** oscillates without returning into the initial state (loop resonance)

total transport stock to the perturbed total production, following the response in total input and total storage. The perturbations seen are caused by the external perturbation. If production sites do not produce, they also do not use commodities for input. Despite this, the total used and total consumption flows do not change as dynamical response to the imposed perturbation. The whole production loss is absorbed by storages. While transport stocks and input flows return to the initial state after the perturbation, reductions of storage contents remain. In analogy to physics, this can be considered as a conservation of damages in the system. In the second article on the description of the Acclimate model, the introduction of enhanced production will break this conservation by introduction of "damage diffusion."

Figure 5a shows the system's response when the storage is sufficient to absorb the loss as damage completely. The upper subplots show the forced deviation of the production strength for the Japanese machinery sector. For 1 day, the global production flow is reduced by 0.8 %. The last row of Fig. 5 shows the total resulting production flow of the network. If we compare the upper and the lowest panel, we see that no cascading production loss was triggered. Since the amount of initial storage is described by a storage fill factor of $\psi_j = 3$ and the perturbed production strength is zero, we can derive that a perturbation period shorter than 3 days is not able to provoke a first cascade.

The subplots between the first and the last show propagation of the perturbation signal within the network and its absorption. Let us treat the forced production loss as an object which is created by perturbation and transported through the network. After production at time t (subplot 1), it is fed into the transport stock (subplot 2), where it is split onto different transportation routes with individual transit time τ. If a part of the production loss exits the transport route, it converts to an input loss (subplot 3) and yields a storage reduction (subplot 4). In the case shown, the initial production loss is small enough to be absorbed completely by storages. The reduction in the used flow attributes to the perturbation only because no used flows are undertaken by production sites that are shutdown. Therefore, no used flow loss (subplot 5) or consumption loss (subplot 6) occurs.

In Fig. 5a, all flow quantities recover eventually to their initial value. The transport stock recovers after all empty sections, which represent losses, propagated along the transport connection to the purchaser. However, global aggregated storages remain on a reduced level. All losses are completely absorbed by storages, and no consumption loss or cascading production loss occurs. Storages that absorb losses do not return to the basic state in this model setup. There is no diffusion mechanism of production loss yet to guarantee the systems evolution into the initial basic state after a finite shock.

In Fig. 5b, the same time series are presented as in Fig. 5b, but for longer perturbation periods, such that the production loss cannot be buffered by storages and cascading losses appear. Alterations of total used flow, total consumption flow, and total production flow appear in Fig. 5b. This spillover, which represents indirect loss, is a direct consequence of the nonsufficient absorption of input loss by storages. Losses are only partially conserved in storages and are captured by consumption sites and production sites. The latter causes further production sites to reduce their production flow. We call such a case cascading production loss, since production loss of one production site represents supply loss for downstream production sites and causes further production decreases. In contrast to damage conservation by storages, cascades of production loss represent an amplification of an original production loss, which act as supply loss. The cascading production loss of a production site represents an amplification of the loss of used flow. The lower bound of the amplification is determined by the added value factor of a production site. The nonlinearity of perfect complementarity, cf. Eq. (5), causes the loss amplification to be even higher. The maximum amplification factor occurs if the supply loss is restricted to the supply commodity i that refers to the smallest flow ratio $U_{i \to js} / \sum_i U_{i \to js}$. The maximum order of cascade, which can be triggered by the perturbation, depends on the perturbation strength, its length, and the size of storages.

A perturbation period of more than 3 days in Fig. 3 triggers production outages of multiply production sites. This cascading loss transfer occurs in the absence of storages or if storages are finished in response to prior supply failures. The dynamic evolution of the production flow after perturbation is shown in Fig. 5b. A perturbation of the global production flow by 0.8 % for day 4–6 causes a global production reduction of 4–6 % for a duration of 3 days starting at day 17. That is an increase in indirect loss by one order of magnitude. Consumption is reduced for 3 days up to 0.35 %. This total production loss represents an enhancement of the direct production loss by factor 4.4.

Figure 5c depicts the response of the system to perturbations, which are long enough to trigger permanent production losses. It seems that production losses once caused by damage can circulate without diffusion in a loop illustrated by Fig. 4.

3.3 Tracking damages and losses along the global supply network: a microscopic perspective

After we have studied the damage/loss propagation of the aggregated stock and flow, we now focus on the propagation of an individual damage/loss, from the perturbed regional sector along the supply chain. For this microscopic perspective, we examine a possible mechanism of loss propagation and illustrate the direct loss and the indirect loss of the first order as a network. This allows us to identify loop constellations in the network, which lead to loss cycles and prevent the production's recovery to the initial state. These cycles can serve as building blocks for the understanding of more complex situations after more realistic perturbations.

Figure 6 schematically illustrates how an externally imposed damage is transferred into production losses and further into supply failures, which might be buffered by storages. If the productive capital of a production site is destroyed, there is no output, from this site which leads to the propagation of loss. Production losses are then propagated to damages in the transport stocks. Transportation delays the damage propagation. If storages of individual production or consumption sites are sufficiently large to completely absorb the input losses, no indirect loss occurs, but storages are reduced (Fig. 6a). If this is not the case, the input losses are transferred to used losses. These might be consumption losses or losses of productive capital inducing production reductions of other production sites (Fig. 6b). Those production losses can then again lead to production losses if the storages of their purchasing production sites are sufficiently small. This cascading behavior reoccurs until all losses are absorbed by storages or captured by consumption sites.

The computed network of direct losses and cascading indirect losses of 1st order are illustrated in Fig. 7. Black arrows represent direct losses, and indirect losses are displayed in red. The width of each flow scales with the size of loss and only the largest 100 losses are shown. All direct losses are caused by the perturbed "Machinery" sector in Japan. The largest losses affect the consumption sites in Japan, which are denoted FNDM here for final demand. At the right-hand side of Fig. 7, the consumption sites are clustered. The abbreviations of the countries and sectors are explained in Tables 3 and 4.

In our simulation, indirect losses of second order, i.e., production losses of production sites that are connected via two links to the perturbed production site, lead to circulating losses in the network. Figure 5c displays the oscillation of aggregated quantities in the global supply network. Those oscillations are caused by resonances of supply failures in the network and depend on the network structure and the corresponding transportation times. Figure 8 illustrates an example configuration that allows circulation of losses due to the absence of any dissipation after a single outage of sector ir.

Consider the setup of production sites ir, jr and is, which is illustrated in Fig. 8. For simplicity, we assume that these production sites are not equipped with storage capacities.

Fig. 6 Damage propagation in the global supply network induced by the breakdown of the perturbed production site. Disturbed production sites (*triangle*) and damaged stocks (*boxes*) are *white filled*. Available stocks (*boxes*) of commodities and nondisturbed production sites (*triangle*) are *black filled*. Direct production losses can be absorbed, if storages are sufficiently large (**a**). Indirect production and consumption losses occur if storages are not sufficiently large (**b**). Transport stocks delay the propagation of supply failures and storages buffer them
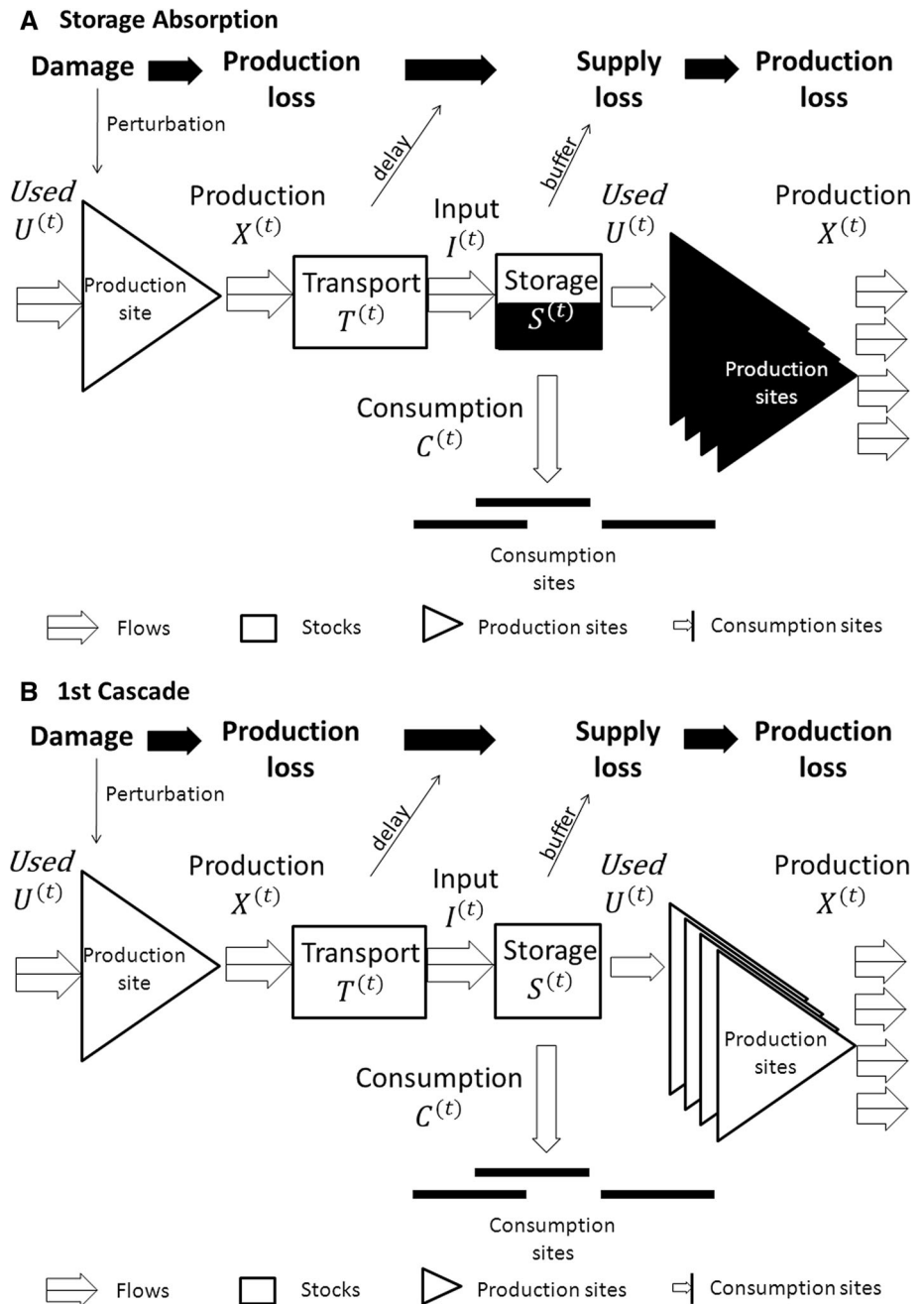
The configuration implies that commodity j is delivered exclusively for ir and js by site jr. Further, production sites ir and is deliver the same amount of good i to jr, i.e., they are equally important for jr. Now we stop the production of production site ir in Fig. 8 for an entire day at time t. Consequently, the input of commodity i for production site jr is half the initial value at time $t + \tau_1$ (note that production site is still delivers commodity i to production site jr). At time $+\tau_1$, jr produces only 50 % of the initial amount of good j and the production of ir and is reduced to 50 % of its initial value at time $t + \tau_1 + \tau_2$ and $t + \tau_1 + \tau_3$,

respectively. Now, there is a supply disruption of both suppliers for jr. If those supply disruption occur synchronized, i.e., $\tau_1 + \tau_2 = \tau_3 + \tau_4$, jr's input and production are reduced to half of its initial value. This reduced production reoccurs with a period of $\tau_1 + \tau_2$. Otherwise, the production equals the initial value. There is no stable oscillating reduction of jr's production if the condition $\tau_1 + \tau_2 = \tau_3 + \tau_4$ is not fulfilled. In such case, supply of commodity i from supplier ir and is does not disrupt simultaneously. In other words, there is no resonance of different supply disruptions.
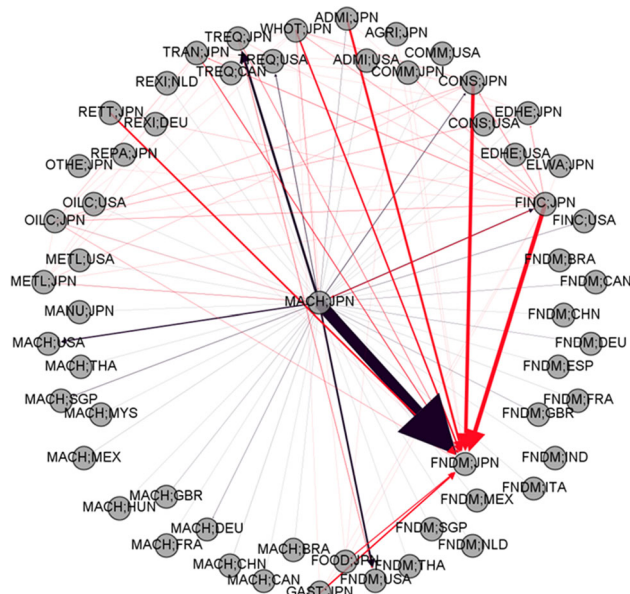
Fig. 7 Direct (*black*) and indirect (*red*) supply shortages after a shutdown of "Machinery" in Japan (centered node). The *arrows* represent supply losses between production or consumption sites. The largest 100 losses are displayed, and the width of arrows scales with the magnitude of loss. The *largest arrows* point to the final demand sector of Japan. Acronyms of sectors and regions are explained in Tables 3 and 4, respectively

In the model setup that we chose, resonances let losses circulate inside the network without diffusion. For more realistic simulations, it will be important to extend this model in a way that losses and damages can be diluted.

3.4 Critical perturbation for the initiation of loss cascades

In this subsection, we examine critical length of perturbation periods necessary for a given production perturbation to trigger cascades of different orders or loop resonances.

Direct damages are imposed on production sites with an external perturbation ratio, $0 \le \lambda_{ir}^{(t)} \le 1$, where unity represents full production and zero a total shutdown. The resulting direct production loss amounts to

$$X_{ir}^{loss} = \int_{t'}^{t'+t_f} dt X_{ir}^* \lambda_{ir}^{(t)}, \tag{18}$$

where t' is the point in time at which the perturbation starts and t_f is its duration. We examine now the critical perturbation length of a cascading response initiation, $t_f^{(casc)}$, and for loop resonance, $t_f^{(loop)}$, as illustrated in Fig. 3. Storages have the capacity to buffer supply failures partially or fully. If the storage is sufficiently large, supply failures can be absorbed and thus maintain the functionality of the production and consumption sites, as illustrated in Fig. 6a.

Table 3 List of all sectors and its acronyms used in the multi-regional input–output table of the EORA project

Acronym	Sector
AGRI	Agriculture
FISH	Fishing
MINQ	Mining and quarrying
FOOD	Food & beverages
TEXL	Textiles and wearing apparel
WOOD	Wood and paper
OILC	Petroleum, chemical and nonmetallic mineral products
METL	Metal products
MACH	Electrical and machinery
TREQ	Transport equipment
MANU	Other manufacturing
RECY	Recycling
ELWA	Electricity, gas and water
CONS	Construction
REPA	Maintenance and repair
WHOT	Wholesale trade
RETT	Retail trade
GAST	Hotels and restaurants
TRAN	Transport
COMM	Post and telecommunications
FINC	Financial intermediation and business activities
ADMI	Public administration
EDHE	Education, health and other services
HOUS	Private households
OTHE	Others
REXI	Re-export and re-import
FNDM	Final demand

3.4.1 Cascading production loss

Below a perturbation length, storages are not depleted completely, and therefore, full absorption of supply failures is ensured. For simplicity, we assume here that all commodities are storable goods including service commodities. Consider a system with an initial ratio between storage and input flows of

$$\psi = \frac{S_i^*}{I_i^*}, \tag{19}$$

which is homogenous for all goods i described by the storage input factor ψ. We estimate the lower limit of the critical perturbation length, in the case of exclusive supply, i.e., only one supplier. In this case, the purchased output of commodity i equals the input of i,

$$X_{ir \to js}^* \le I_{i \to js}^* \to X_{ir \to js}^* = I_{i \to js}^*. \tag{20}$$

The critical perturbation length $t_f^{(casc)}$ is

Table 4 List of all regions and its acronyms used in the multi-regional input–output table of the EORA project

Acronym	Region	Acronym	Region	Acronym	Region
AFG	Afghanistan	PYF	French Polynesia	NER	Niger
ALB	Albania	GAB	Gabon	NGA	Nigeria
DZA	Algeria	GMB	Gambia	NOR	Norway
AND	Andorra	GEO	Georgia	PSE	Palestine
AGO	Angola	DEU	Germany	OMN	Oman
ATG	Antigua and Barbuda	GHA	Ghana	PAK	Pakistan
ARG	Argentina	GRC	Greece	PAN	Panama
ARM	Armenia	GRL	Greenland	PNG	Papua New Guinea
ABW	Aruba	GTM	Guatemala	PRY	Paraguay
AUS	Australia	GIN	Guinea	PER	Peru
AUT	Austria	GUY	Guyana	PHL	Philippines
AZE	Azerbaijan	HTI	Haiti	POL	Poland
BHS	Bahamas	HND	Honduras	PRT	Portugal
BHR	Bahrain	HKG	Hong Kong	QAT	Qatar
BGD	Bangladesh	HUN	Hungary	KOR	South Korea
BRB	Barbados	ISL	Iceland	MDA	Moldova
BLR	Belarus	IND	India	ROU	Romania
BEL	Belgium	IDN	Indonesia	RUS	Russia
BLZ	Belize	IRN	Iran	RWA	Rwanda
BEN	Benin	IRQ	Iraq	WSM	Samoa
BMU	Bermuda	IRL	Ireland	SMR	San Marino
BTN	Bhutan	ISR	Israel	STP	Sao Tomé and Príncipe
BOL	Bolivia	ITA	Italy	SAU	Saudi Arabia
BIH	Bosnia &Herzegovina	JAM	Jamaica	SEN	Senegal
BWA	Botswana	JPN	Japan	SRB	Serbia
BRA	Brazil	JOR	Jordan	SYC	Seychelles
VGB	British Virgin Islands	KAZ	Kazakhstan	SLE	Sierra Leone
BRN	Brunei	KEN	Kenya	SGP	Singapore
BGR	Bulgaria	KWT	Kuwait	SVK	Slovakia
BFA	Burkina Faso	KGZ	Kyrgyzstan	SVN	Slovenia
BDI	Burundi	LAO	Laos	SOM	Somalia
KHM	Cambodia	LVA	Latvia	ZAF	South Africa
CMR	Cameroon	LBN	Lebanon	ESP	Spain
CAN	Canada	LSO	Lesotho	LKA	Sri Lanka
CPV	Cap Verde	LBR	Liberia	SUR	Suriname
CYM	Cayman Islands	LBY	Libya	SWZ	Swaziland
CAF	Central African Republic	LIE	Liechtenstein	SWE	Sweden
TCD	Chad	LTU	Lithuania	CHE	Switzerland
CHL	Chile	LUX	Luxembourg	SYR	Syria
CHN	China	MAC	Macao	TWN	Taiwan

$$t_f^{(\text{casc})} = \psi \left(1 - \lambda_{ir}^{(t)} \right)^{-1}. \tag{21}$$

A perturbation period below the critical perturbation length $t_f^{(\text{casc})}$ prevents all production sites in the global supply network to suffer from supply losses.

Figure 6b illustrates the case of cascading production failure if the perturbation length is longer than $t_f^{(\text{casc})}$. All storages are depleted while supply failure continuous.

Perfect complementarity forces further production site to stop production. The lower limit of the critical perturbation length of the first cascade is given by $t_f^{(\text{casc})}$, and we can generalize it for the nth cascade

$$t_f^{(\text{casc},n)} = n\psi(1 - \lambda_{ir}^{(t)})^{-1}. \tag{22}$$

We allow now the diversification of supply, i.e., there is no exclusive supply between production sites. Assume that all production sites js have the same ratio,
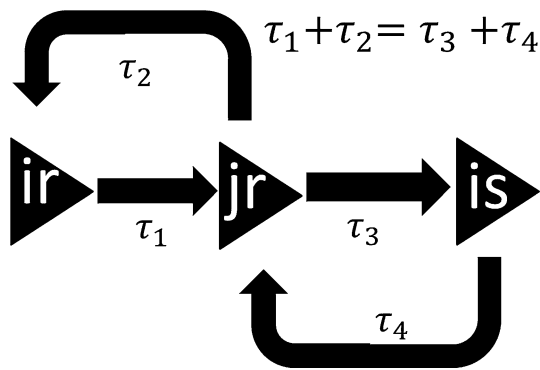
Fig. 8 An idealized example scenario to illustrate circulating losses. A one-time failure of *ir* with a perturbation length that leads to complete storage depletions of good *i* of *jr* and good *j* of *ir* and is causes *jr* to fail periodically

$$\frac{X^*_{ir \to js}}{I^*_{i \to js}} = R = \text{const}, \tag{23}$$

of purchased supply and input for commodity *i*, then Eq. (22) becomes

$$t_f^{(\text{casc},n)} = n\psi(1 - \lambda_{ir}^{(t)})^{-1} R^{-1}. \tag{24}$$

An absence of supply diversification, i.e., $R = 1$, minimizes the length of the perturbation period, with respect to diversification, needed to trigger the nth cascade. If the supply of one commodity *i* is not homogenously diversified, $R \neq \text{const}$, we can only give a lower bound for the minimal critical length of the perturbation period,

$$t_f^{(\text{casc},n)} \geq n\psi \left(1 - \lambda_{ir}^{(t)}\right)^{-1}, \tag{25}$$

as a necessary condition for production losses of nth order. In Fig. 3c, the cascades are superimposed onto the resonances caused by the supply loops discussed above.

3.4.2 Cyclic production loss

Above a critical perturbation length, the global production ratio does not return into the initial value, but oscillates. The right panel of Fig. 3 shows the ratio of mean production to initial production for the given setup. In this model version, production losses are not able to diffuse out of the system and circulate in the network for infinitive time. This circulation of loss is only possible if all storages that are located along the circulation pathway are completely depleted in the aftermath of the perturbation. If storage contents were available, losses would be absorbed either completely or partially. In the latter case, a remaining loss would keep circulating. Supply chains always build up cycles if the global supply network is finite and output flows are never exclusively sent to consumption sites. We provide now some elementary constellations that

can result in cyclic behavior in order to provide building blocks for the understanding of more complex situations.

The simplest possible circulation pathway (loop) for a loss consists of two flows between 2 production sites. One flow from a perturbed production site *ir* to another one *js* and a second flow that directs back to the perturbed production site *ir* (cf. Figure 8). If all production sites and consumption sites are equipped with the same S^*/I^* ratio with no diversified supply, then the critical perturbation period to establish a two-connection loop is

$$t_{f,c}^{(l=2)} = 2\psi(1 - \lambda_{ir}^{(t)})^{-1}. \tag{26}$$

This perturbation length ensures that storages of two production sites are finished, and any further loss would circulate freely in the loop. This condition does not exclude larger loops. Those are possible with parallel arrangements of two-connection loops. The simulation setting of Fig. 3 with $\psi = 3$ and an inhomogeneous diversification structure shows that the smallest perturbation period above $t_{f,c}^{(l=2)} = 6$, i.e., 7 days, is causing production losses to circulate in the system for infinitive time.

The circulating supply failure, described in the previous section, only occurs for existing exclusive supply. However, oscillating production losses might appear. That happens if supply failures of the same commodity, i.e., diversified supplier, occur in resonance as shown in Fig. 8.

4 Conclusion

We present here the basic version of the numerical model for global damage propagation, Acclimate, which describes the dynamics of global spread of local disasters along economic supply chains on a daily to monthly time scale. We connect production and consumption sites to a global network using multi-regional input–output tables. The different production and consumption sites are modeled as agents with a distinct decision rational. This yields a propagation dynamics for perturbation of the basic state on this network. The transportation is modeled with geographically motivated transit times. Production and consumption sites are equipped with storages for input goods.

Acclimate is developed to model the propagation of supply losses in the wake of an outage of production sites, induced for example by extreme weather events. In Sect. 3, we investigated diagnostically how a locally limited destruction of production sites induces damage transfers depending on the strength of the perturbation and the buffer capacities.

We investigated in Sect. 3.1 deviations in the total production level of the network in response to different durations of the breakdown. We observed in case of a

collapse of the "Machinery" sector in Japan that the given global network structure shows different response behavior. Global percussions occur if storage capacities are sufficiently low or if the perturbation period is sufficiently long. Furthermore, circulating losses in the network arise for a sufficiently strong perturbation.

To understand those phenomena, we interpreted in Sect. 3.2 the global supply network as a stock and flow model and resolved the dynamics for the different quantities that describe the entire system. In that way, we could study the causal dependencies between the various stock and flow quantities. In addition, we observed that after a disaster, in the absence of loss circulation, all quantities return to their initial values except the storage content that remains at a reduced level. This conservation of supply loss in storage stocks can be explained by the absence of diffusion mechanisms in the model at this stage.

In contrast to Sect. 3.2, where we investigated the dynamics of aggregated quantities, we studied in Sect. 3.3 how the perturbation signal transfers along concrete supply chains. We show the direct and first-order cascading losses for an outage of the "Machinery" sector in Japan.

Finally, in Sect. 3.4, we assumed idealized networks with homogenous input storage fill factors $\psi_{i \to js}$ for all agents and found critical length of perturbation periods that lead to cascading losses of nth order or continuously circulating losses.

At this stage, we presented the pure forward supply disruption propagation dynamics. In order make the model more realistic and applicable to real disaster scenarios, reasonable storage sizes have to be set for the various sectors and the model should be extended by various features. Demand dynamics will be implemented in Wenz et al. (2014b) together with the possibility of production extensions. We intend to extend the model at a later stage by a decision structure based on the price dynamics and a responding restructuring, which reflects an evolution of the network.

References

Andrew RM, Peters GP (2013) A multi-region input–output table based on the global trade analysis project database (GTAP-MRIO). Econ Syst Res 25:99–121. doi:10.1080/09535314.2012.761953

Auffhammer M, Ramanathan V, Vincent JR (2006) Integrated model shows that atmospheric brown clouds and greenhouse gases have reduced rice harvests in India. Proc Natl Acad Sci USA 103:19668–19672. doi:10.1073/pnas.0609584104

Bouwer L, Crompton R (2007) Confronting disaster losses. Sci NY 318:753

Bridges T, Kovacs D, Wood M (2013) Climate change risk management: a Mental Modeling application. Environ Syst Decis 33(3):376–390

Brzoska M, Scheffran J (2013) Climate and war: no clear-cut schism. Nature 498:171. doi:10.1038/498171c

Ciscar Martinez JC, Feyen L, Soria Ramirez A et al (2014) Climate Impacts in Europe. The JRC PESETA II Project. Institute for Prospective and Technological Studies, Joint Research Centre

Dietzenbacher E, Los B, Stehrer R et al (2013) The construction of world input–output tables in the WIOD project. Econ Syst Res 25:71–98. doi:10.1080/09535314.2012.761180

Emanuel K (2011) Global warming effects on US hurricane damage. Weather Clim Soc 3(4):261–268

Greenberg M, Lahr M, Mantell N (2007) Understanding the economic costs and benefits of catastrophes and their aftermath: a review and suggestions for the US federal government. Risk Anal 27(1):83–96

Haddad E, Okuyama Y (2012) Spatial propagation of the economic impacts of bombing: the case of the 2006 war in Lebanon (No. 2012_19). University of São Paulo (FEA-USP).

Haddad E, Teixeira E (2013) Economic impacts of natural disasters in megacities: the case of floods in São Paulo, Brazil. ERSA conference paper

Hallegatte S (2008) An adaptive regional input-output model and its application to the assessment of the economic cost of Katrina. Risk Anal 28:779–799. doi:10.1111/j.1539-6924.2008.01046.x

Hallegatte S (2012) Economics: the rising costs of hurricanes. Nat Clim Change 2:148–149. doi:10.1038/nclimate1427

Helbing D (2013) Globally networked risks and how to respond. Nature 497:51–59. doi:10.1038/nature12047

Hsiang S, Burke M (2014) Climate, conflict, and social stability: what does the evidence say? Clim Change 123(1):39–55

Hsiang S, Burke M, Miguel E (2013) Quantifying the influence of climate on human conflict. Science 341(6151):1235367

IPCC (2012) Managing the risks of extreme events and disasters to advance climate change adaptation. In: Field CB, Barros V, Stocker TF, Qin D, Dokken DJ, Ebi KL, Mastrandrea MD, Mach KJ, Plattner G-K, Allen SK, Tignor M, Midgley PM (eds) A special report of working groups I and II of the intergovernmental panel on climate change. Cambridge University Press, Cambridge

IPCC (2013) Climate change 2013: the physical science basis: contribution of working group I to the fifth assessment report of the intergovernmental panel on climate change

IPCC (2014) Climate change 2014: impacts, adaptation, and vulnerability. Part A: global and sectoral aspects. In: Field CB, Barros VR, Dokken DJ, Mach KJ, Mastrandrea MD, Bilir TE, Chatterjee M, Ebi KL, Estrada YO, Genova RC, Girma B, Kissel ES, Levy AN, MacCracken S, Mastrandrea PR, White LL (eds) Contribution of working group II to the fifth assessment report of the intergovernmental panel on climate change. Cambridge University Press, Cambridge

Kajitani Y, Tatano H (2014) Estimation of production capacity loss rate after the great east japan earthquake and Tsunami in 2011. Econ Syst Res 26:13–38. doi:10.1080/09535314.2013.872081

Lenton T, Ciscar J (2013) Integrating tipping points into climate impact assessments. Clim Change 117(3):585–597

Lenzen M, Kanemoto K, Moran D, Geschke A (2012) Mapping the structure of the world economy. Environ Sci Technol 46:8374–8381. doi:10.1021/es300171x

Levermann A (2014) Climate economics: make supply chains climate-smart. Nature 506:27–29. doi:10.1038/506027a

Levermann A, Bamber JL, Drijfhout S et al (2011) Potential climatic transitions with profound impact on Europe. Clim Change 110:845–878. doi:10.1007/s10584-011-0126-5

Linkov I, Varghese A, Jamil S (2005) Multi-criteria decision analysis: a framework for structuring remedial decisions at contaminated sites. In: Linkov I, Ramadan AB (eds) Comparative risk assessment and environmental decision making. Springer, Netherlands, pp 15–54

Linkov I, Bridges T, Creutzig F et al (2014) Changing the resilience paradigm. Nat Clim Change 4:407–409. doi:10.1038/nclimate2227

Mendelsohn R, Emanuel K, Chonabayashi S, Bakkensen L (2012) The impact of climate change on global tropical cyclone damage. Nat Clim Change 2:205–209. doi:10.1038/nclimate1357

Moss RH, Edmonds JA, Hibbard KA et al (2010) The next generation of scenarios for climate change research and assessment. Nature 463:747–756. doi:10.1038/nature08823

Narayanan B, Aguiar A, McDougall R (2012) Global trade, assistance, and production: the GTAP 8 data base, Center for Global Trade Analysis, Purdue University

Okuyama Y (2008) Critical review of methodologies on disaster impacts estimation. Background paper EDRR report

Okuyama Y, Santos JR (2014) Disaster impact and input–output analysis. Econ Syst Res 26:1–12. doi:10.1080/09535314.2013.871505

Peters GP, Andrew R, Lennox J (2011) Constructing an environmentally-extended multi-regional input–output table using the GTAP database. Econ Syst Res 23:131–152. doi:10.1080/09535314.2011.563234

Rahmstorf S, Coumou D (2011) Increase of extreme events in a warming world. Proc Natl Acad Sci USA 108:17905–17909. doi:10.1073/pnas.1101766108

Rose A (2004) Defining and measuring economic resilience to disasters. Disaster Prev Manag 13:307–314. doi:10.1108/09653560410556528

SEARATES LP (2014) Distances and transit time. www.searates.com/reference/portdistance. Accessed 11 Feb 2014

Strazzo S, Elsner JB, Trepanier JC, Emanuel KA (2013) Frequency, intensity, and sensitivity to sea surface temperature of North Atlantic tropical cyclones in best-track and simulated data. J Adv Model Earth Syst 5:500–509. doi:10.1002/jame.20036

Tukker A, de Koning A, Wood R et al (2013) Exiopol—development and illustrative analyses of a detailed global MR EE SUT/IOT. Econ Syst Res 25:50–70. doi:10.1080/09535314.2012.761952

Wenz L, Willner S, Bierkandt R et al (2014a) An inhomogeneous approximate-and-update approach to refine multi-regional input-output tables. Econ Syst Res. doi:10.1080/09535314.2014.987731

Wenz L, Willner S, Bierkandt R, Levermann A (2014b) Acclimate—a model for economic damage propagation. Part II: a dynamic formulation of the backward effects of disaster induced production failures in the global supply network. Environ Syst Decis. doi:10.1007/s10669-014-9521-6

World Bank (2012) Turn down the heat—why a 4 C warmer world must be avoided. World Bank, Washington. http://documents.worldbank.org/curated/en/2012/11/17097815/turn-down-heat-4%C2%B0c-warmer-world-must-avoided

Zhai AR, Jiang JH (2014) Dependence of US hurricane economic loss on maximum wind speed and storm size. Environ Res Lett 9:064019. doi:10.1088/1748-9326/9/6/064019